



Article scientifique

Article

2009

Published version

Open Access

This is the published version of the publication, made available in accordance with the publisher's policy.

Molecular imaging by micro-CT: specific E-selectin imaging

Wyss, Caroline; Schaefer, Stephan C.; Juillerat-Jeanneret, Lucienne; Lagopoulos, Lucienne; Lehr, Hans-Anton; Becker, Christoph; Montet, Xavier Cédric Rodolphe

How to cite

WYSS, Caroline et al. Molecular imaging by micro-CT: specific E-selectin imaging. In: European radiology, 2009, vol. 19, n° 10, p. 2487–2494. doi: 10.1007/s00330-009-1434-2

This publication URL: <https://archive-ouverte.unige.ch/unige:20182>

Publication DOI: [10.1007/s00330-009-1434-2](https://doi.org/10.1007/s00330-009-1434-2)

Caroline Wyss
Stephan C. Schaefer
Lucienne Juillerat-Jeanneret
Lucienne Lagopoulos
Hans-Anton Lehr
Christoph D. Becker
Xavier Montet

Molecular imaging by micro-CT: specific E-selectin imaging

Received: 9 October 2008
Revised: 10 March 2009
Accepted: 23 March 2009
Published online: 14 May 2009
© European Society of Radiology 2009

C. Wyss · S. C. Schaefer ·
L. Juillerat-Jeanneret · L. Lagopoulos ·
H.-A. Lehr
University Institute of Pathology,
Centre Hospitalier Universitaire
Vaudois,
Lausanne, Switzerland

C. D. Becker · X. Montet (✉)
Department of Radiology,
University of Geneva,
Micheli-du-Crest 24,
1211 Geneva, Switzerland
e-mail: xavier.montet@hcuge.ch
Tel.: +41-22-379-5784
Fax: +41-223795260

X. Montet
Department of Cell Physiology
and Metabolism, University of Geneva,
Geneva, Switzerland

Abstract The primary goal of this study was to design a fluorescent E-selectin-targeted iodine-containing liposome for specific E-selectin imaging with the use of micro-CT. The secondary goal was to correlate the results of micro-CT imaging with other imaging techniques with cellular resolution, i.e., confocal and intravital microscopy. E-selectin-targeted liposomes were tested on endothelial cells in culture and in vivo in HT-29 tumor-bearing mice ($n=12$). The liposomes contained iodine (as micro-CT contrast medium) and fluorophore (as optical contrast medium) for confocal and intravital microscopy. Optical imaging methods were used to confirm at the cellular level, the observations made with micro-CT. An ischemia-reperfusion model was used to trigger neovessel formation for intravital imaging. The E-selectin-

targeted liposomes were avidly taken up by activated endothelial cells, whereas nontargeted liposomes were not. Direct binding of the E-selectin-targeted liposomes was proved by intravital microscopy, where bright spots clearly appeared on the activated vessels. Micro-CT imaging also demonstrated accumulation of the targeted liposomes into subcutaneous tumor by an increase of 32 ± 8 HU. Hence, internalization by activated endothelial cells was rapid and mediated by E-selectin. We conclude that micro-CT associated with specific molecular contrast agent is able to detect specific molecular markers on activated vessel walls in vivo.

Keywords Micro-computed tomography · Molecular imaging · E-selectin · Liposomes

Introduction

Molecular imaging, i.e., the measurement and/or imaging of biological processes in living organisms at the molecular and cellular level, is now part of the preclinical world and even part of the clinical world for imaging modalities such as positron-emission tomography [1]. Previous reports have already proved that molecular imaging is feasible by nuclear medicine [2], magnetic resonance [3, 4] and optical [5] imaging. Micro-computed tomography (micro-CT) has not been used widely in this field. The addition of this imaging technique into the molecular world will expand the molecular “toolbox” and hence the possibilities of research. We present here proof that micro-CT, associated

with specific contrast media, is able to detect the presence of specific molecular markers on activated endothelial cells. More specifically, we chose to target E-selectin expression on activated endothelial cells.

E-selectin (also known as CD62E) is an inducible cell-adhesion molecule belonging to the C-type lectin family [6]; it is expressed on the surface of endothelial cells in response to inflammatory processes [7] or on proliferating endothelial cells [8], but not on quiescent cells. Hence, the differential expression of E-selectin between activated and nonactivated cells makes E-selectin an optimal candidate for molecular imaging. Targeting E-selectin will allow specific imaging of activated vessels. Peptides that specifically bind to E-selectin [7, 9] were selected from a

recombinant peptide library and showed affinity in the low nanomolar range [7].

Previous studies have demonstrated that iodinated liposomes are useful contrast media for micro-CT [10, 11]. As liposomes are composed of uni- or bilamellar membranes entrapping contrast media (iodine in case of micro-CT), we postulated that post-insertion of specific targeting moieties into the membrane of liposomes should be possible, as previous work on targeted liposomes has already been published [12, 13]. Hence, we have synthesized iodinated liposomes targeting the expression of E-selectin on activated endothelial cells and applied this contrast media to detect the expression of E-selectin on activated endothelial cells by micro-CT imaging.

Materials and methods

Synthesis of the E-selectin-targeted liposomes and iodinated unilamellar liposomes

E-selectin-binding peptide (ESBP) with the following sequence (FITC)BCDSDSDITW-DQLWDLMK (B stands for beta-alanine, FITC for fluorescein) was purchased from Tufts University (Tufts University, Boston, MA, USA).

To synthesize E-selectin-targeted liposomes (Fig. 1), 100 μ l of 1 mM 1,2-distearoyl-sn-glycerol-3-phosphoethanolamine-N-[amino(polyethylene glycol)-2000] (DSPE-PEG-2000, Avanti Polar Lipids) was activated with 100 μ l of 150 mM succinimidyl iodoacetate (SIA; Molecular Biosciences, CO, USA) in dimethylsulfoxide (DMSO), and the mixture was allowed to stand at room temperature for 30 min. The ESBP was then added to 1.25 mg peptide in 100 μ l DMSO, and the mixture was allowed to stand overnight at room temperature. The resulting ESBP-DSPE-PEG-2000 was purified twice through exclusion chromatography (PD10 column, GE Healthcare, Otelfingen, Switzerland) in phosphate buffer saline (PBS). Then the

ESBP-DSPE-PEG-2000 was post-inserted in 4 ml iodinated liposomes by gentle stirring overnight to generate ESBP-liposomes. Fluorescent DSPE-PEG-2000 was obtained by covalently binding NHS ester of indocyanin 3.5 (Cy3.5) according to the manufacturers' instructions (Amersham Biosciences, Piscataway, NJ, USA) and was purified twice by exclusion chromatography and post-inserted in 4 ml iodinated liposomes. The fluorescence of the FITC on the ESBP allowed quantification of the peptide/DSPE-PEG-2000 liposome ratio. The average number of peptides post-inserted into liposomes was determined spectrophotometrically from fluorescein absorbance at 493 nm [14] using a concentration of 1.25×10^{13} liposomes/ml, and the average number of Cy3.5 post-inserted into liposomes was determined from its absorption at 580 nm. The size of the various liposomes was determined by laser light scattering (Zetasizer, Malvern Instruments, Malvern, PA, USA).

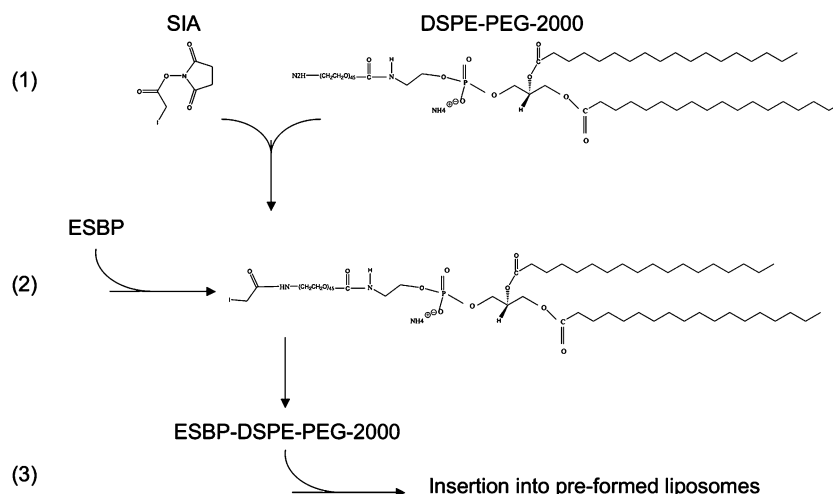
Iodinated unilamellar liposomes (BR22, 400 ± 50 nm diameter as determined by laser light scattering), prepared by a film/extrusion method as described previously [15], were provided by Bracco Research (Bracco Research, Plan-les-Ouates, Geneva, Switzerland). To avoid leakage of the iodine due to equilibration of the internal and external phases, iodine [Iomeprolum; (N,N-bis (2,3-dihydroxypropyl)-5-[(hydroxy-acetyl)-methylamino]-2,4,6-tri-iodo-1,3 benzene-dicarboxamide)], Bracco Switzerland, Switzerland) was also present in the external phase. These unilamellar liposomes entrapped 70 mg iodine/ml equilibrated with 287 mg iodine/ml in the external phase. Nontargeted iodinated liposomes were used as control.

In vitro analysis

Confocal microscopy

To study the specificity of ESBP-liposomes, EC219 cells were grown on histological slides.

Fig. 1 Synthesis of ESBP-liposomes. DSPE-PEG-2000 was first activated with succinimidyl iodoacetate (SIA) (1). The terminal NH₂ group of DSPE-PEG-2000 was reacted with the NHS ester of the SIA. Then, the lateral sulfhydryl group of the cysteine (second amino acid of the ESBP) was reacted with the iodoacetyl group of the activated DSPE-PEG-2000 (2) to form a covalent bond between the ESBP and the DSPE-PEG-2000. The resulting ESBP-DSPE-PEG-2000 was then inserted into preformed iodinated liposomes (3)



Activation of the cells was undertaken through stimulation with 200 U/ml mouse TNF- α and 50 U/ml rat IFN- γ (Roche Diagnostic, Mannheim, Germany) over a 24-h period. Nonactivated cells served as control.

ESBP-liposomes (200 μ l of the stock solution, corresponding to 14 mg iodine) were added to nonactivated and cytokine-activated cells for 4 h, then rinsed twice with PBS and fixed for 5 min in buffered 4% formaldehyde. Cells were then rinsed twice in PBS and mounted in immunomount (Thermo Shandon, Pittsburgh, PA, USA). Imaging was performed on a Leica SP5 confocal microscope (Leica Microsystems, Wetzlar, Germany) using filters of 580 (excitation)/610 (emission). Activation of the cells was proved by an increase in NO synthesis, as previously published [19].

In vivo analysis

Two types of models of neovessel formation were used in this study. The first one consisted of an ischemia-reperfusion model, which was used for intravital microscopy (see below). The second one consisted of tumor neovessel formation, which was used for micro-CT imaging.

Animal preparation for intravital microscopy

All the experiments using mice were approved by the local ethics committee and followed the Swiss guidelines for animal experiments.

The dorsal skinfold chamber preparation in five awake C57BL/6 mice (Janvier, le Genest-St-Isle, France) was used for intravital microscopy. The experimental preparation used in this study was very similar to that described previously [16]. Briefly, C57BL/6 mice were fed standard rodent diet and allowed water ad libitum; they were anesthetized by injection of ketamine 100 mg/kg IP (Ketavet, Pharmacia, Erlangen, Germany) and xylazine 20 mg/kg IP (Rompun, Bayer, Leverkusen, Germany). Two titanium frames were implanted so as to sandwich the extended double layer of the skin. One layer of the skin was completely removed in an 18-mm-diameter circular area, and the remaining layer, consisting of epidermis, subcutaneous tissue, and a thin striated skin muscle, was covered with a coverslip incorporated in one of the frames. The dorsal skinfold chambers were well tolerated by the animals, i.e., they showed no signs of discomfort and no adverse effects on feeding and sleeping habits.

Ischemia-reperfusion

An ischemia model was used to trigger neovessel formation. The experimental protocol was performed as described

previously [17]. A 2-h period of ischemia was induced by application of gentle pressure on the muscle against a coverslip with a silicone pad and an adjustable screw that was just sufficient to empty the blood vessels [17].

Intravital fluorescence microscopy

Between the implantation of the observation chamber and the microscopic investigation, a recovery period of 72–96 h was allowed to eliminate the effects of anesthesia and surgical trauma on the microvasculature. Epi-illumination (100-W xenon lamp attached to an Axiotech intravital microscope, Zeiss, Jena, Germany) and a 20 \times water immersion objective (total magnification 560 \times ; Zeiss) were used to select 10 regions of interest per chamber, each containing ≥ 1 venule of various diameters. Awake animals were then imaged in bright field and fluorescence imaging before and after intravenous (iv) injection of 400 μ l of either ESPB-liposomes or liposomes. Postinjection images were taken immediately after injection as well as after 1 and 2 h. The microscopic images were recorded with a high-resolution black-and-white camera (Kappa, Gleichen, Germany) on DVD video.

All animals were euthanized after the last imaging session with a single injection of KCl (200 mEq/kg).

Animal model for micro-CT

Cell culture

The human colon adenocarcinoma cell line HT-29 was obtained from LGC Promochem (LGC Promochem, France). Cells were cultured in McCoy's 5a medium modified with 1.5 mM L-glutamine and adjusted to contain 2.2 g/L sodium bicarbonate and 10% heat-inactivated fetal bovine serum (all from GIBCO, Invitrogen, Switzerland), and grown at 37°C in a humidified 5% CO₂ atmosphere.

In vivo studies

Athymic female nude mice (Janvier, le Genest-St-Isle, France) weighing 20–25 g were used in this study. Gas anesthesia (isoflurane 1–2%) was used during all injection of contrast media, as well as during all surgical procedures and micro-CT imaging sessions. Both ESPB-liposomes and nontargeted iodinated liposomes were injected through the tail vein of the animals.

Tumor-bearing animals

After anesthesia (isoflurane 1–2%) and local disinfection, tumor cells were injected subcutaneously (1 million cells in

50 μ l PBS) into the left and right paralumbar regions. Tumor cells were allowed to grow for 5–6 days and then imaged with a micro-CT after injection of 400 μ l ESBP-liposomes ($n=6$) or 400 μ l liposomes ($n=6$), corresponding to 28 mg of iodine. All animals were euthanized after the last imaging session with a single injection of KCl (200 mEq/kg).

Micro-CT acquisition

All images were acquired on a Skyscan-1076 micro-CT (Skyscan, Aartselaar, Belgium). All in vivo micro-CT examinations were acquired at 35- μ m resolution using the following parameters: 65 kV anode voltage, 180 μ A, 1.4° rotation step, 316 ms exposure time per view. A 0.5-mm aluminum filter was installed in the beam path to cut off the softest x-rays in order to increase the accuracy of the beam-hardening correction (BHC). These settings allowed scanning an entire mouse at 35- μ m resolution in 30 min [each mouse received an estimated dose of 0.7 Gy during the image acquisition (data from the manufacturer)]. All animals were imaged before and immediately after injection of the probes and after 1, 2, 4, 6, 8, and 24 h.

Image reconstruction and analysis

Cross-sectional images were reconstructed using a classical Feldkamp cone-beam algorithm [18]. The corrected image data were calibrated into the conventional linear scale of CT number, known as Hounsfield units (HU), defined so that water and air have values of 0 and -1,000 HU, respectively.

Regions of interests (ROIs) were manually drawn to assess attenuation coefficients in HU in the blood-filled chamber of the left and right ventricles, as well as in the tumor. A monoexponential fit of the signal measured in the blood-filled chambers of the heart gave the blood half-life of the different contrast media. The enhancement of the tumor over time was also assessed.

Statistical analysis was performed with Prism 4 (GraphPad Prism, version 4a, 2003, GraphPad Software, San Diego, CA, USA). Data are reported as mean \pm standard error (SE). Significance was determined using Mann-Whitney test; P values < 0.05 were considered significant.

To compare different groups, ANOVA analysis was used. When a significant P value was found ($P < 0.05$), a Bonferroni's post-test correction was performed.

Histology

All tumors were excised, snap frozen, and cut into 7- μ m sections using a CM3050 cryostat (Leica Microsystems,

Germany). Sections were stained with hematoxylin-eosin (HE). Immunohistochemistry was conducted on acetone-fixed cryosections, which were blocked with PBS containing 0.5% donkey serum and 2% BSA, and incubated for 1 h with the ESBP peptide at 1 μ g/ml and rat anti-mouse CD31 diluted 1:200 (Molecular Probes, Invitrogen, Switzerland). A secondary antibody (donkey anti-rat; TexasRed, Jackson ImmunoResearch Europe) was applied at 1:500 for 1 h. Nuclear staining was obtained with a mounting medium containing DAPI (Vectashield hard set with DAPI, Vector Laboratories, Burlingame, CA, USA).

Results

ESBP-liposomes characterization

The average size of the liposomes used in this study was 400 nm. The average number of peptides inserted into preformed liposomes, determined spectrophotometrically, was 1,492 ESBP per liposomes. The average number of Cy3.5 molecules per liposome was 120.

Activation of endothelial cells

Activation of endothelial cells with TNF- α and IFN- γ was verified through their production of nitric oxide (NO), as previously published [19]. Activated endothelial cells produced 5.3 μ M NO per 72 h, whereas control cells (nonactivated) produced 0.05 μ M NO per 72 h.

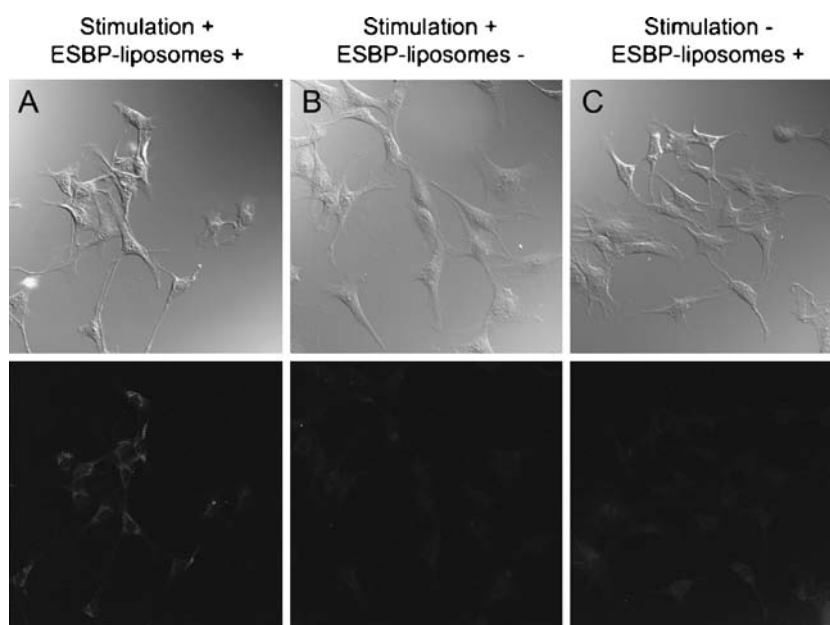
Confocal imaging

The specificity of the interaction of ESBP-liposomes with E-selectin in vitro was examined by confocal microscopy on cytokine-activated and nonactivated cells. Nonactivated cells showed almost no binding of the ESBP-liposomes, whereas activated cells showed accumulation of the ESBP-liposomes visible throughout the cytoplasm as punctuated centers of fluorescence. Stimulated cells without ESBP-liposomes (used as control) showed no fluorescence (see Fig. 2).

Intravital microscopy

All the implanted dorsal chambers were of good quality and permitted image acquisition. The acquisition of images before administration of the ESBP-liposomes or liposomes showed no fluorescence inside the vessels (see Fig. 3a and d). Immediately after iv administration of the contrast media, a clear fluorescent signal was present in the plasma (see Fig. 3b and e), but no accumulation was detected in the

Fig. 2 Confocal microscopy. Phase contrast images (*top row*) as well as fluorescence imaging (*bottom row*) are shown. Cytokine-activated endothelial cells incubated with ESBP-liposomes showed a clear cytoplasmic signal (**a**), whereas activated endothelial cells without ESBP-liposomes showed none (**b**). Nonactivated endothelial cells incubated with ESBP-liposomes showed almost no intracellular signal (**c**)



vessel walls. Two hours after injection of the ESBP-liposomes, bright spots accumulated in the walls of veins, whereas there was no bright signal on the arterioles (see Fig. 3c). The control probe (liposomes without targeting) showed no accumulation on the vessel wall (see Fig. 3f).

Tumor implantation and micro-CT imaging

All mice developed small (3–5 mm) tumors after 5–6 days. All micro-CT acquisitions were of good quality and allowed for blood half-life calculations of the probes (see Fig. 4a and c) as well as for tumor imaging (see Fig. 4b and d). Blood half-lives of the ESBP-liposomes and liposomes

were $121 (\pm 11)$ and $71 (\pm 18)$ min, respectively. Small subcutaneous tumors were easily visible and showed greater enhancement after injection of ESBP-liposomes than after liposomes (see Fig. 4d). Nontargeted liposomes showed a simple disappearance from the blood, corresponding to the blood half-lives of the probes. In contrast, ESBP-liposomes showed first a binding on the tumor vessels followed by clearing. Enhancement after injection of the probes was different between the two probes at 120, 240, and 360 min with ESBP-liposomes being trapped in the tumor's vessels for a longer time. The residency time of the ESBP-liposomes inside the tumor was 314 ± 2 min, whereas residency time for nontargeted liposomes was only 90 ± 1 min ($P < 0.001$).

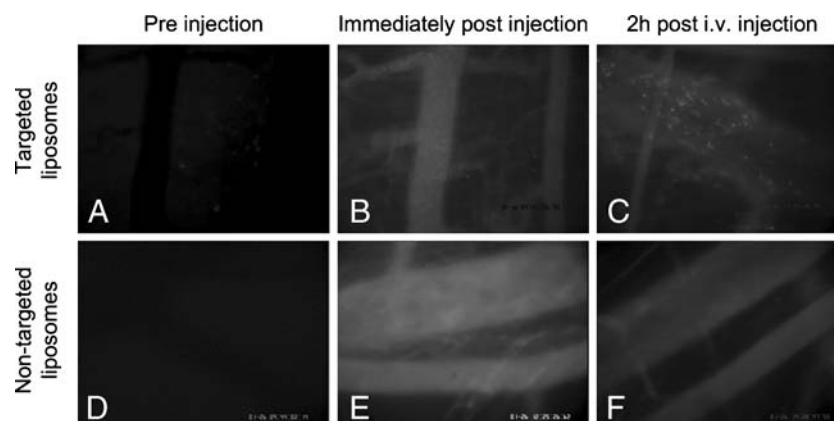


Fig. 3 Intravital microscopy. Low background signal was observed on intravital microscopy (**a** and **d**). The plasma became highly fluorescent after intravenous injection of either ESBP-liposomes (**b**) or nontargeted liposomes (**e**). Two hours after the iv injection, bright

spots appeared when ESBP-liposomes were injected (**c**), whereas no fluorescent signal was seen when nontargeted liposomes were injected (**f**). Note that the majority of bright spots appearing after injection of ESBP-liposomes are located on the postcapillary veins

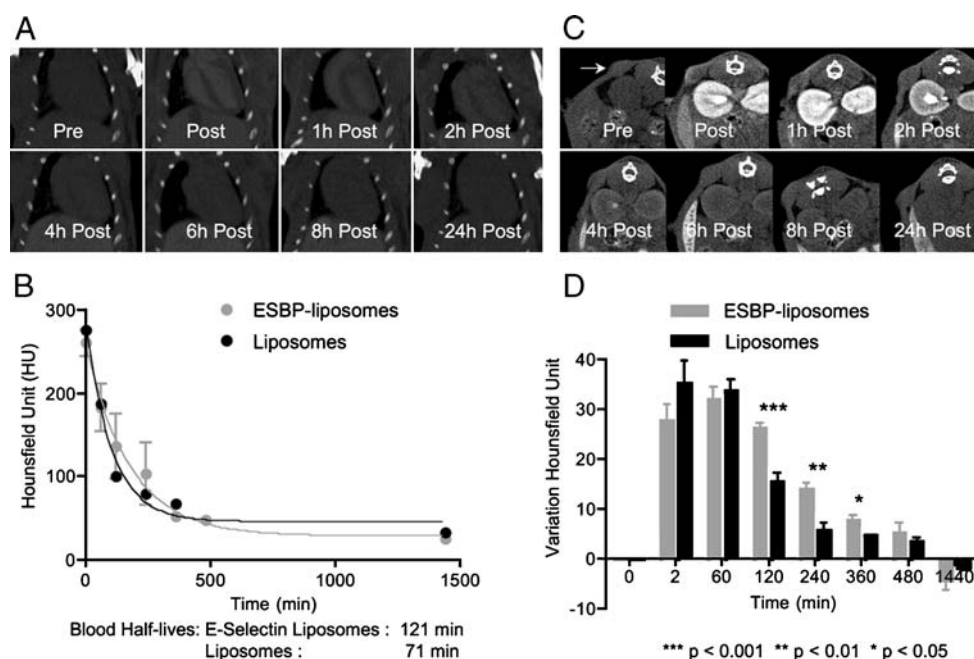


Fig. 4 In vivo micro-CT imaging. Determination of the blood half-lives of the compounds. Heart cavities were used to generate signal (in Hounsfield units) versus time (a). A monoexponential fit (b) allowed the blood half-lives of the ESBP-liposomes (121 min) and nontargeted liposomes (71 min) to be calculated. This difference in blood half-lives was not statistically significant ($P=0.24$). Acquisition of the micro-CT images in the tumor region (c) showed a clear

enhancement of the subcutaneous tumor (arrow). The evolution of the density of the tumor versus time is presented (d) for the ESBP-liposomes as well as for the nontargeted liposomes. Differences between the two contrast media reached statistical difference at 120, 240, and 360 min. ESBP-liposomes accumulated in the tumor, whereas nontargeted liposomes disappeared from the blood

Histology

Hematoxylin and eosin staining confirmed the presence of small tumors in all animals (see Fig. 5). Immunohistochemistry showed a good colocalization between ESBP and CD31.

Discussion

Molecular imaging has already been demonstrated with nuclear medicine, MRI, and optical imaging. Micro-CT has never been used to directly interrogate molecular markers on the surface of cells. This study demonstrates that the use of micro-CT, combined with targeted liposomes directed against E-selectin expression on activated endothelial cells, enables direct imaging of this receptor.

E-selectin is expressed on activated endothelial cells and plays important roles in leukocyte rolling during inflammatory processes or angiogenesis [20, 21]. Moreover, as E-selectin is expressed on the surface of activated endothelial cells, an intravenous injection allows the E-selectin-targeted contrast medium to be in direct contact with its molecular target without the need to extravasate. The liposomes used in this study have a diameter of 400 nm. This relatively big size makes the liposomes an intravas-

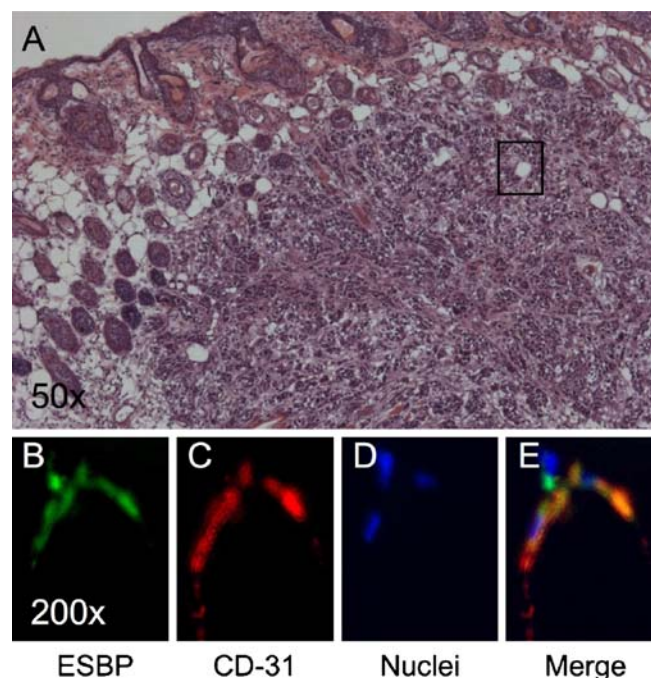


Fig. 5 Correlative histology. Hematoxylin and eosin staining (a) of the subcutaneous tumor. Immunohistochemistry against E-selectin (b), CD31 (c), and DAPI staining of the nuclei (d), as well as merge (e) are presented. The histology confirmed the presence of E-selectin on the endothelial cells (colocalization with CD31)

cular contrast medium, with no chance for the compound to pass through the endothelial barrier [22]. At the same time, the size also increases the blood half-life of the compound [10], which gives more time for the targeted compound to interact with its molecular target. Hence, liposomes of such size are ideal candidates for molecular imaging of intravascular targets. The use of smaller liposomes would be necessary to reach extravascular targets. The general principle of extravasation and uptake of microparticles into cells through endocytic routes is now well accepted. Discussion in many review articles suggests that, for this process to occur efficiently, particle sizes need to be less than 100 nm [22]. Synthesis of small liposomes (as small as 50 nm) has already been published [23, 24]. Such small liposomes should be able to extravasate from neovessels and reach extravascular targets. Future studies are needed to evaluate the utility of such a compound for molecular imaging.

The targeting moiety used in this study (ESBP) is known to be specific for E-selectin [5], with a high affinity constant, on the order of a few nanomoles [7]. Our *in vitro* experiments (confocal microscopy) indicate that quiescent endothelial cells do not bind to the targeted liposomes, whereas activated cells do (see Fig. 2).

Our *in vivo* experiments (intravital microscopy and micro-CT imaging) indicate that targeted liposomes accumulate in the veins where the endothelium has been activated, whereas nontargeted liposomes do not (see Figs. 3 and 4). Intravital microscopy, which was performed on awake mice, clearly shows bright spots on the postcapillary veins, but not on the arterial wall. This finding is consistent with previous results showing that E-selectin binding is more potent at low flow [25].

In vivo accumulation of the targeted ESBP-liposomes into subcutaneous tumors was proved by micro-CT imaging. Micro-CT offers extremely high-resolution images with good contrast among air, bone, fat, and soft tissue, but suffers from inherently poor contrast among soft tissues. Hence, injection of exogenous contrast medium is mandatory to differentiate soft tissue by micro-CT [10, 11]. One of the most used exogenous contrast media in the clinics is iodine, which absorbs x-rays efficiently. The presence of iodine in a voxel of the image induces x-ray absorption and an increase in density. Hence, accumulation of ESBP-liposomes into the tumor induces an increase in density. The kinetics of accumulation of the ESBP-liposomes is also different from that of the nontargeted one. ESBP-liposomes first show an accumulation over 60 min, corresponding to

progressive binding, then a slow decrease, whereas nontargeted liposomes show a monoexponential decay, corresponding to the blood half-lives of the compound.

Competition or blocking experiments have not been performed because of the difficulties in displacing a multivalent compound [12]. The affinity of multivalent compounds is higher than their monovalent counterpart. Hence their displacement is virtually impossible by classical competition or blocking experiments.

Study limitation

Biodistribution of the E-selectin-targeted liposomes was not assessed in this study because it was outside the scope of the primary goal. Nevertheless, biodistribution should be studied in the future, if one wants to use this compound. Toxicity of the compounds was also not tested, but we do not expect any toxicity of the compounds because the iodinated liposomes have already been in phase II clinical study and the adjunction of a small peptide should not be toxic.

Despite the use of two animal models (ischemia-reperfusion for intravital microscopy and implanted tumors for micro-CT imaging), we believe this paper clearly demonstrated (1) the binding of the targeted compounds at a cellular resolution (by confocal microscopy), (2) the binding of the targeted compounds to activated vessels *in vivo* (by intravital microscopy) and (3) the binding of the targeted compounds to activated vessels in tumor (by micro-CT).

Conclusions

This study demonstrates that micro-CT, associated with targeted iodinated liposomes can identify a molecular target on the endothelium, enabling the realization of molecular imaging.

Acknowledgements This work was supported by the Swiss National Science Foundation (grant number: 320000-116813). The authors also thank the Ernst and Lucie Schmidheiny Foundation and the Geneva Academic Society and the Swiss Commission for Technology and Innovation (CTI/KTI; project No 7985.2 LSPP-LS) for financial support. The authors also thank Dr. Jean-Yves Chatton from the Cellular Imaging Facility (CIF, Lausanne, Switzerland) for help during the acquisition of confocal microscopy pictures.

References

1. Weissleder R (2002) Scaling down imaging: molecular mapping of cancer in mice. *Nat Rev Cancer* 2:11–18
2. Blankenberg FG, Strauss HW (2007) Nuclear medicine applications in molecular imaging: 2007 update. *Q J Nucl Med Mol Imaging* 51:99–110
3. Montet X, Montet-Abou K, Reynolds F et al (2006) Nanoparticle imaging of integrins on tumor cells. *Neoplasia* 8:214–222

4. Montet X, Weissleder R, Josephson L (2006) Imaging pancreatic cancer with a peptide-nanoparticle conjugate targeted to normal pancreas. *Bioconjug Chem* 17:905–911
5. Funovics M, Montet X, Reynolds F et al (2005) Nanoparticles for the optical imaging of tumor E-selectin. *Neoplasia* 7:904–911
6. Stoolman LM (1989) Adhesion molecules controlling lymphocyte migration. *Cell* 56:907–910
7. Martens CL, Cwirla SE, Lee RY et al (1995) Peptides which bind to E-selectin and block neutrophil adhesion. *J Biol Chem* 270:21129–21136
8. Bischoff J, Brasel C, Kraling B et al (1997) E-selectin is upregulated in proliferating endothelial cells in vitro. *Microcirculation* 4:279–287
9. Zinn KR, Chaudhuri TR, Smyth CA et al (1999) Specific targeting of activated endothelium in rat adjuvant arthritis with a ^{99m}Tc-radiolabeled E-selectin-binding peptide. *Arthritis Rheum* 42:641–649
10. Montet X, Pastor CM, Vallee JP et al (2007) Improved visualization of vessels and hepatic tumors by micro-computed tomography (CT) using iodinated liposomes. *Invest Radiol* 42:652–658
11. Mukundan S Jr, Ghaghada KB, Badea CT et al (2006) A liposomal nanoscale contrast agent for preclinical CT in mice. *AJR Am J Roentgenol* 186:300–307
12. Elbayoumi TA, Torchilin VP (2008) Liposomes for targeted delivery of antithrombotic drugs. *Expert Opin Drug Deliv* 5:1185–1198
13. Saad M, Garbuzenko OB, Ber E et al (2008) Receptor targeted polymers, dendrimers, liposomes: which nanocarrier is the most efficient for tumor-specific treatment and imaging? *J Control Release* 130:107–114
14. Montet X, Funovics M, Montet-Abou K et al (2006) Multivalent effects of RGD peptides obtained by nanoparticle display. *J Med Chem* 49:6087–6093
15. Fouillet X, Tournier H, Khan H et al (1995) Enhancement of computed tomography liver contrast using iomeprol-containing liposomes and detection of small liver tumors in rats. *Acad Radiol* 2:576–583
16. Schafer SC, Sehr DN, Kamler M et al (2005) Paradoxical attenuation of leukocyte rolling in response to ischemia-reperfusion and extracorporeal blood circulation in inflamed tissue. *Am J Physiol Heart Circ Physiol* 289:H330–H335
17. Lehr HA, Guhlmann A, Nolte D et al (1991) Leukotrienes as mediators in ischemia-reperfusion injury in a microcirculation model in the hamster. *J Clin Invest* 87:2036–2041
18. Feldkamp L, Davis L, Kress J (1984) Practical cone-beam algorithm. *J Opt Soc Am A* 1:612–619
19. Murata J, Corradin SB, Janzer RC et al (1994) Tumor cells suppress cytokine-induced nitric-oxide (NO) production in cerebral endothelial cells. *Int J Cancer* 59:699–705
20. Austrup F, Vestweber D, Borges E et al (1997) P- and E-selectin mediate recruitment of T-helper-1 but not T-helper-2 cells into inflamed tissues. *Nature* 385:81–83
21. Graves BJ, Crowther RL, Chandran C et al (1994) Insight into E-selectin/ligand interaction from the crystal structure and mutagenesis of the lec/EGF domains. *Nature* 367:532–538
22. Garnett MC, Kallinteri P (2006) Nanomedicines and nanotoxicology: some physiological principles. *Occup Med (Lond)* 56:307–311
23. Chono S, Tauchi Y, Morimoto K (2006) Influence of particle size on the distributions of liposomes to atherosclerotic lesions in mice. *Drug Dev Ind Pharm* 32:125–135
24. Verma DD, Verma S, Blume G et al (2003) Particle size of liposomes influences dermal delivery of substances into skin. *Int J Pharm* 258:141–151
25. Ley K, Tedder TF (1995) Leukocyte interactions with vascular endothelium. New insights into selectin-mediated attachment and rolling. *J Immunol* 155:525–528